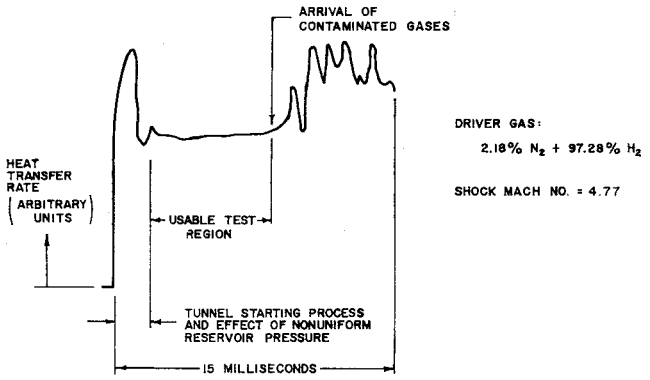

Fig. 3 Test section stagnation-point heat-transfer rate record showing arrival of test gas that has been contaminated and heated by combustion products.

with the cooler uncontaminated test air. Now the time required for these hotter mixed gases to reach the nozzle entrance will depend on the length of the slug of test gas. This is apparent when one compares the runs near $M_s = 6.0$ with the runs near $M_s = 4.7$. For the $M_s = 6.0$ runs, the hot combustion products have not affected the test section airflow velocity 3 msec after shock reflection (run 8), but they have affected the airflow velocity 4.5 msec after shock reflection (run 3). When a less energetic driver, which is produced by diluting hydrogen with nitrogen and which should tailor (in the absence of interface combustion) at about $M_s = 4.7$, is used, the hot combustion gases affect the test-section airflow sometime between 7 and 11 msec after shock reflection (runs 9 and 10). The arrival of the hot gases in the test section is illustrated nicely in Fig. 3. There it is seen that the heat-transfer rate in the test section remains nearly constant until about 10 msec after the arrival of the starting shock wave. After that, it goes up sharply, indicating the arrival of the test gas that has been contaminated and heated by the combustion products.

Of course, contamination of test air by driver gas also takes place when interface combustion is absent (e.g., with a helium driver).[9] However, under tailored-interface conditions without the interface combustion, the driver-gas contamination is more difficult to detect.

So far, technical difficulties have prevented direct velocity measurement when conditions for tailored-interface operation (again, in the absence of interface combustion) were achieved at a shock Mach number near 10 (obtainable in the HIT only by use of an isochoric combustion driver). However, for this case, the amount of hydrogen not consumed in our particular isochoric driver combustion process is about 8% of the total driver mixture, and the reservoir pressure records again show evidence of combustion at the interface. Because of the decreased length of the slug of useful test air at these higher shock Mach numbers, it is expected that the test air will be contaminated by the combustion products at a very early time.

Conclusions

When using a driver containing as little as 8% hydrogen to drive air in a shock tube, combustion takes place at the interface. Initially, because of this interface combustion, pressure waves are generated which perturb shock-tunnel reservoir conditions. These effects can be accounted for by assuming the process is isentropic and calculating the reservoir enthalpy change from the measured pressure change. However, the hot combustion products mix into the test gas and change both its state and composition, thus limiting its usefulness for testing. The time it takes for this contaminated air to first reach the test section decreases rapidly with increasing shock Mach number. Thus, in most cases, this interface mixing, rather than phenomena that can be described on a wave diagram in terms of pressure waves, will limit the usable test time of shock tunnels.

References

[1] Copper, J. A., "The hypervelocity impulse tunnel: facility description and expected performance," Douglas Aircraft Co., Inc., Rept. SM-41377 (November 1962).

[2] Cunningham, B. E. and Kraus, S., "Experimental investigation of the effect of yaw on rates of heat transfer to transverse circular cylinders in a 6500-foot-per-second hypersonic airstream," NACA TM A58E19 (August 26, 1958).

[3] Karamcheti, K., Vall, W., Kyser, J. B., and Rasmussen, M. L., "Measurements of pressure and speed of flow in a spark-heated hypersonic wind tunnel," Arnold Engineering Development Center TDR 62-218 (November 1962).

[4] Skinner, G. T., "Analog network to convert surface temperature to heat flux," Cornell Aeronautical Lab. Rept. CAL-100 (February 1960).

[5] Wittliff, C. E., Wilson, M. R., and Hertzberg, A., "The tailored-interface hypersonic shock tunnel," J. Aerospace Sci. **26**, 219–228 (1959).

[6] Copper, J. A., "Experimental investigation of the equilibrium interface technique," Phys. Fluids **5**, 844–849 (1962).

[7] Copper, J. A., Akamine, E., Hameetman, F. J., Miller, H. R., and Ogostalick, E. J., "Hypervelocity techniques and measurements," Douglas Aircraft Co., Inc., Rept. SM-43056-5 (January 1964).

[8] Flagg, R. F., "Advances in shock tunnel driving techniques," *Advanced Experimental Techniques for Study of Hypervelocity Flight, Proceedings of the Third Hypervelocity Techniques Symposium* (Denver Research Institute, Denver, Colo., 1964), pp. 89–115.

[9] Bird, K. D., Martin, J. F., and Bell, T. J., "Recent developments in the use of the hypersonic shock tunnel as a research and development facility," *Advanced Experimental Techniques for Study of Hypervelocity Flight, Proceedings of the Third Hypervelocity Techniques Symposium* (Denver Research Institutute, Denver, Colo., 1964), pp. 7–50.

Correlation of Motor and Strand Composite Propellant Burning Rate

L. E. Herrington*
Aerojet-General Corporation, Sacramento, Calif.

THE burning rate of composite propellants measured in the Crawford Bomb testing of uncured liquid strands may be correlated with data from small motors by the following equation:

$$P/r_n = (b_n/b_s)P/r_s + K_0 \quad (1)$$

where

r = linear burning rate
P = pressure
b_n/b_s = slope
K_0 = intercept
s = as subscript, strand properties
n = as subscript, motor properties

Equation (1) states that the ratio of pressure to burning rate for the motor and strand can be related by two parameters that are independent of pressure when the ratios are

Presented as Preprint 64-150 at the AIAA Solid Propellant Rocket Conference, Palo Alto, Calif., January 29–31, 1964; revision received June 12, 1964. The guidance provided by B. E. Paul in the development of this work is gratefully acknowledged. Appreciation is also expressed to J. H. Wiegand and A. E. Lemke for their support in this study. Informative discussions with N. S. Cohen regarding Summerfield's theory and the combustion of metals in propellants are also acknowledged.

* Chemical Engineer, Propellant Ballistics Department.

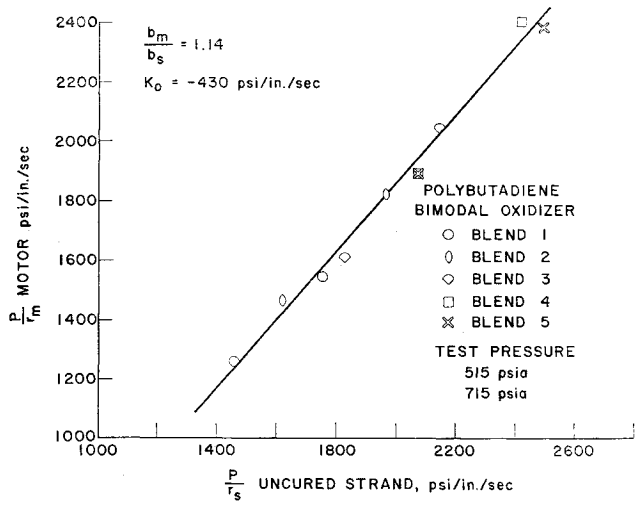

Fig. 1 Correlation of motor and strand ratio of pressure to burning rate (five blends of two oxidizer grinds).

measured at corresponding pressures. The steady-state motor design equation is given by

$$P/r = \rho A_w/C_w A_t \tag{2}$$

where

ρ = propellant density
A_w = burning area
C = mass flow coefficient
A_t = nozzle throat area

Therefore, Eqs. (1) and (2) allow the motor design parameters and strand burning rate to be directly related.

Equation (1) was derived from Summerfield's equation for the granular diffusion flame model.[1] This flame model, which was developed by Summerfield, resulted in a two parameter equation relating the pressure and burning rate of composite propellant of the ammonium perchlorate type to the processes of diffusion and chemical reaction in the flame zone. To utilize this theory for correlating motor and strand burning rates, it must first be assumed that both burning rates can be represented by the model. Differences in the two types of burning must be attributed to differences in the reaction and diffusion effects in the respective flame zone. The pressure dependence of the motor and strand rate can then be written separately as

$$1/r_s = (a_s/P) + (b_s/P^{1/3}) \tag{3}$$

$$1/r_n = (a_n/P) + (b_n/P^{1/3}) \tag{4}$$

where

a = reaction time parameter
b = diffusion time parameter

Equation (1) can be obtained by multiplying Eq. (3) by the ratio b_n/b_s, subtracting from Eq. (4) and multiplying the results through by the pressure P. When the final results are placed in the form of Eq. (1), the slope of the correlation between the ratios of pressure to burning rate is seen to represent the ratio of the motor and strand diffusion time parameters. The intercept K_0 is found to be

$$K_0 = a_n - (b_n/b_s)a_s \tag{5}$$

Equation (5) shows how the intercept of Eq. (1) depends upon the reaction and diffusion parameter.

By maintaining the identity of the model in the correlation process, a valuable improvement over earlier empirical correlations is obtained. The behavior of the model parameters has been previously studied and characterized. Although it was pointed out that absolute values of the reaction and diffusion time parameters depended upon the proportionality constant between the heat flux to the propellant surface and the burning rate, Summerfield and co-workers showed the theoretical and experimental dependence of the model parameters upon the flame temperature and oxidizer particle size.[2] The reaction time parameter a was found to increase when the oxidizer to fuel ratio was altered to obtain a cooler flame. This was in keeping with the inverse dependence of a upon the gaseous reaction rate between the oxidizer and fuel. The model predicted that the parameter a was independent of the oxidizer particle size when the fuel to oxidizer ratio remained fixed. Experimental support of this effect was not conclusive, although it remained as a possibility. Under the condition of a fixed oxidizer to fuel ratio the diffusion time parameter b did increase with the oxidizer particle size. Thus the sensitivity of the b parameter to the oxidizer particle size was in the direction predicted by the proposed diffusion mechanism. The lack of sensitivity of b to flame temperature was also predicted by the model and measured experimentally.

The effect of strand size on combustion efficiency for aluminized propellants was reported by McCarty.[3] Small strands were found to be lower in efficiency because of the escape of unburned metal particles into the surrounding inert gas atmosphere. Thus, flame temperature will necessarily be lower in the strand flame zone. This lower temperature should have certain predictable effects upon Eq. (1). For example, because the diffusion parameter b is not very sensitive to temperature, the quantity b_n/b_s should be near unity. The intercept given by Eq. (5) should be negative because of a larger reaction time parameter in the strand resulting from a decrease in the gaseous reaction rate.

The most important aspect of Eq. (1) is that the Summerfield model correctly predicts that the slope and intercept are not dependent upon the oxidizer particle size. Since the diffusion time parameters are both proportional to the same property of the oxidizer particle size, the ratio b_n/b_s should not depend upon this property even when the individual b values vary widely. In addition, predicted insensitivity of the reaction time parameter a to a change in oxidizer size indicates that the value of the intercept given by Eq. (5) will not change.

The invariance of the slope and intercept of Eq. (1) to wide changes in the average oxidizer particle size has been verified by experimental data. Figures 1 and 2 show two aluminized polybutadiene formulations with high solids loadings. Changes in oxidizer size were obtained by the blending together of various proportions of different oxidizer grinds. Figure 1 represents the data from five mixes prepared from two oxidizer grinds. The ratios of pressure to burning rate

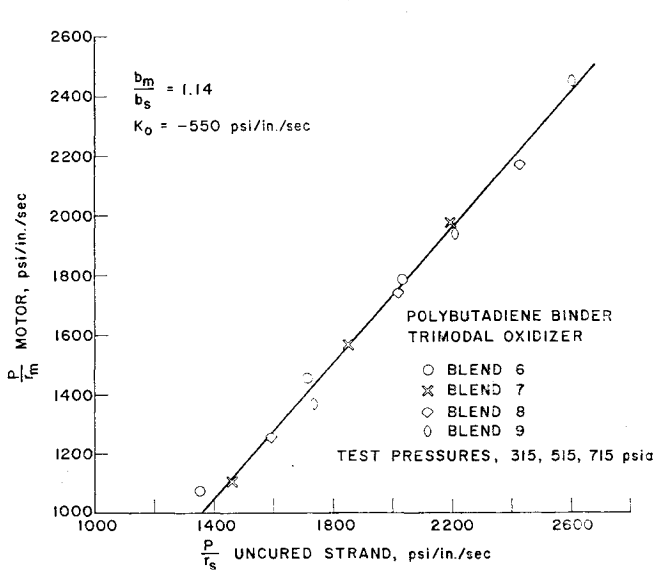

Fig. 2 Correlation of motor and strand ratio of pressure to burning rate (four blends of three oxidizer grinds).

were measured at pressures of 515 and 715 psia. A slope of 1.14 and intercept of −430 lb-sec/in.^{3} were obtained from a straight line fit of the data. Figure 2 shows the results obtained from four mixes with different blends of three oxidizer grinds. Burning rates were measured at pressures of 315, 515, and 715 psia. A straight line through the data gave a slope of 1.14 and intercept of −550 lb-sec/in.^{3}.

The slopes and intercepts for fits of small motor and liquid strand data to Eq. (1) have been measured for both polyurethane and polybutadiene formulations. Data precision of 2% or better has resulted. The observed scatter has been largely attributable to the small motors. Formulations not containing burning-rate catalyst have yielded slopes ranging between 1.12 and 1.18, with intercepts ranging between −350 and −550 lb-sec/in.^{3}. Therefore, the trends predicted by the Summerfield Granular Diffusion Model have been verified experimentally. More economical motor design through increased application of strand burning rates can be achieved through the use of Eq. (1).

References

[1] Summerfield, M., Sutherland, G. S., Webb, M. J., Taback, H. J., and Hall, K. P., "Burning mechanism of ammonium perchlorate propellants," *ARS Progress in Astronautics and Rocketry: Solid Propellant Rocket Research*, edited by M. Summerfield (Academic Press, New York, 1960), Vol. 1, pp. 141–160.

[2] Blair, D. W., Bastress, E. K., Hermance, L. E., Hall, K. P., and Summerfield, M., "Some research problems in the steady state burning of composite solid propellants," *ARS Progress in Astronautics and Rocketry: Solid Propellant Rocket Research*, edited by M. Summerfield (Academic Press, New York, 1960), Vol. 1, pp. 183–206.

[3] McCarty, K. P., "Techniques for studying the combustion of aluminum in solid propellant," Pyrodynamics **1**, no. 1, 71–87 (1964).

Electric Propulsion Characteristics of a Pulsed Plasma Rail Accelerator

DANIEL H. WINICUR*

Hughes Aircraft Company, El Segundo, Calif.

Nomenclature

x = axial displacement of plasma slug
t = time
l = rail electrode length
$2r$ = rail electrode width
d = distance to one rail electrode from centerline of the other rail electrode
I = electric current
V = voltage
C = capacitance
R = resistance
L = inductance
B = magnetic field along the plasma slug caused by the current flowing in the rail conductors
v = plasma velocity
m = mass per pulse
T = discharge time
g_0 = gravity constant
μ_0 = magnetic permeability of a vacuum
F = instantaneous force on plasma slug
E = stored energy per plasma slug mass
s = total length of plasma column
ds = increment of plasma column length
K = magnetic field strength per unit current acting on plasma
I_T = total impulse per pulse
I_{sp} = specific impulse
Pe = accelerator jet power
(P/F) = specific power
η = power efficiency
ΔV = net velocity increment

Subscript

0 = power supply circuit element

Superscripts

$(\ )'$ = value per unit or rail length
$(\bar{\ })$ = averaged quantity

Received October 14, 1963; revision received May 22, 1964.

* Member of the Technical Staff, Space Systems Division. Associate Member AIAA.

THIS note presents the results of an analog computer study of the electric propulsion characteristics of a confined pulsed plasma rail accelerator. The rail accelerator has been proposed for long duration space propulsion missions such as attitude control, orbit raising, and deep space propulsion.[1–3] The theory and operation of this accelerator is amply described in Refs. 1–6.

The "plasma slug model" has been used with variable rail resistance and inductance. The propellant is assumed to be injected in a compact form with the plasma remaining as a slug. This plasma slug is then treated as a moving circuit element of negligible resistance.[3] Assuming that the motion of the plasma slug can be described one-dimensionally,

$$dL/dt = (dL/dx)(dx/dt) = L'v \tag{1}$$

where dL/dx is assumed to be a constant equal to L', the rail inductance per unit length.

Starting with the expression for the instantaneous force on a column of plasma moving in a direction normal to the current flowing through it,

$$F = I \int_s B\, ds \tag{2}$$

Maes[1] has derived the following equation for F which includes the force due to the current flowing in the back conductors, parallel to the plasma slug, in addition to the force due to the current flowing through the parallel rail electrodes:

$$F = -\frac{\mu_0 I^2}{2\pi}\left\{\frac{(x^2+d^2)^{1/2}}{x} + \ln\left[\frac{x+(r^2+x^2)^{1/2}}{x+(d^2+x^2)^{1/2}}\right] + \ln\frac{d}{r} - 1\right\} \tag{3}$$

When $x \gg d$, i.e., when the effect of the back conductors is negligible, this reduces to the familiar expression

$$F = \tfrac{1}{2}L'I^2 \tag{4}$$

After integrating Eq. (3) from $x = 0$ to $x = l$ to obtain the space average of F, the instantaneous force on the plasma can be expressed as

$$F = KI^2 \tag{5}$$

The coefficient K is a constant dependent only on the accelerator geometry equal to the magnetic field strength per unit current acting on the plasma column.

The time varying resistance and inductance are then expressed in terms of R' and L':

$$R = R'x \qquad L = L'x \tag{6}$$

Equation (5) is combined with the Kirchhoff voltage equation of the equivalent electrical current to yield the equation governing the current flowing in the rails:

$$0 = \frac{1}{C_0}\int_0^t I\,dt + \left[L_0 + \frac{L'K}{m}\int_0^t\int_0^t I^2 dt\, dt\right]\frac{dI}{dt} + I\left[R_0 + \frac{R'K}{m}\int_0^t\int_0^t I^2 dt\, dt + \frac{L'K}{m}\int_0^t I^2 dt\right] \tag{7}$$